Supporting Information for

Self-assembled natural small molecules diterpene acids with favorable anticancer activity and biosafety for synergistically enhanced antitumor chemotherapy

Jianjun Cheng [a #], Shiyao Fu [a #], Zhao Qin [a], Ying Han [a], Xin Yang [a *].

[a] School of Chemistry and Chemical Engineering, Harbin Institute of Technology, No. 92 West Dazhi Street, Nan Gang District, Harbin, Heilongjiang.

[#] These authors made equal contributions to this work.

***Corresponding author**. Tel.: +86 451 86403309; Fax: +86 451 86403379.

E-mail address: yangxin@hit.edu.cn (Xin Yang)

Experimental Section

1.1 Materials.

Pinus koraiensis is collected from the Yichun forest area of Heilongjiang Province and identified by Professor Zhenyu Wang who majored in Chinese Medicine classification, Harbin Institute of Technology. A voucher specimen (No. 201466) is deposited at the School of Chemistry and Chemical Engineering, Harbin Institute of Technology, P. R. China. Paclitaxel (PTX, 98%) and polyvinyl alcohol (PVA, Mw=30000-40000) was obtained from Aladdin (Shanghai, China). All reagents were analytical grade, purchased from Fuyu Chemical (Tianjin, China) and used as received. RPMI1640, Penicillin–streptomycin, Trypsin-EDTA Solution, phosphate buffer saline (PBS), and fetal bovine serum (FBS) were purchased from Gibco (USA). 3-(4,5-Dimethylthiazol-2-yl)-2,5-diphenyltetrazolium bromide (MTT) and dimethyl sulfoxide (DMSO) were obtained from Sigma -Aldrich (USA). Breast cancer cells 4T1 and MCF-7 were obtained from Shanghai Cell Bank of Chinese Academy of Sciences.

1.2 Characterization.

The 1D NMR experiments were performed on a Bruker DRX-400 (Rheinstetten, Germany) at 400 MHz. UV–Vis spectra were obtained on a TU-1900 PERSEE spectrometer (Beijing, China). IR spectra were recorded on a Perkin Elmer Spectrum FT-IR spectrophotometer (Waltham, MA, USA) as KBr pellets and the absorption frequencies were expressed in reciprocal centimeters (cm^{-1}). Mass spectral studies were carried out on a Hewlett-Packard 5989B MS (ESI) (Palo Alto, CA, USA). Silica gel (Qingdao, China), reversed-phase silica gel (Kyoto, Japan), Sephadex LH-20 (Boston, MA, USA) were used for column chromatography. Scanning electron microscopy (SEM) images of samples were recorded on a Quanta 200FEG SEM spectrometer at 20 kV (Hillsboro, OR, USA). Particle size and zeta potential of samples were analyzed on Zetasizer Nano ZS 90 (Malvern, UK) at 25℃. The contact angle was recorded with a HARKE-SPCA (Beijing, China).

1.3 PTX loading and encapsulation efficiency.

AA-PTX NPs were first disassembled by dissolving in MeOH and the following sonication. Then the PTX concentration was determined at 227 nm using the HPLC system equipped with an LC-10ADvp pump, an SPD-10Avp UV–Vis detector, and a Diamonsil C18 reversed-phase column (4.6 mm× 250 mm, 5 μm). The mobile phase was acetonitrile/water (65/35, v/v) solutions and the flow rate was 1.0 mL/min. The encapsulation efficiency (EE) and drug loading (DL) were calculated by the following equations:

$$\mathrm{EE}(\%) = \frac{\text{amount of PTX in AA - PTX NPs}}{\text{amount of the feeding PTX}} \times 100\%$$

$$\mathrm{DL}(\%) = \frac{\text{amount of PTX in AA - PTX NPs}}{\text{amount of AA - PTX NPs}} \times 100\%$$

1.4 DFT calculations

Molecular geometry optimizations of four diterpene acids and PTX were carried out by using Gaussian 09 program with density functional theory (DFT) at the B3LYP/6-31G (d, p) level of theory [1].

1.5 *In vitro* drug release.

In vitro drug release profiles of PTX from AA-PTX NPs were determined in PBS at different pH by dialysis method (n=6). As follows, 5mL of AA-PTX NPs suspension (dissolved in PBS) were transferred into dialysis bags (Pierce, USA) with a MWCO of 3500 Da. The dialysis bags were incubated in 1 L of PBS (pH 7.4, 6.7, or 5.6) containing Tween 80 (1%, v/v) at 37°C with the speed of the dissolution apparatus at 100 r/min. At the desired time, the PTX content in the dialysis bag is determined using the HPLC method as described above.

1.6 Cellular uptake of AA-PTX NPs

In the cellular uptake experiment, 4T1 cells (10^5) were seeded in 6-well plates and incubated for 24 h at 37 °C. Then the cells were incubated with fluorescein isothiocyanate (FITC)-labeled AA-PTX NPs (25 μg mL^{-1}) for various periods of time (5 min, 0.5 h, and 3 h). After incubation, fixing and DAPI staining of the cells, then imaged under fluorescent inverted microscope (FIM). Meanwhile, flow cytometric analysis was performed to evaluate the mean fluorescence intensity of cellular uptake. Same as above cell treatments, after incubation with FITC-labeled AA-PTX NPs, the10^4 cells were analyzed with the Guava EasyCyte mini system.

1.7 Hemolysis

The hemolytic test was performed using fresh red blood cells collected from BALB/c mice. Erythrocytes were collected by centrifugation at 3000 rpm for 5 min, then washed five times with PBS to remove the white blood cells from the surface until the supernatant is clear. Subsequently, the cells were diluted with PBS to prepare 2% (v/v) red cell suspension for further use. AA NPs and AA-PTX NPs were dispersed in RBC suspensions at gradient concentrations (nanoparticles: erythrocyte suspension=1:1), then incubated at 37 °C for 3 h, and centrifuged at 3000 rpm for 10 min. The absorption values of the supernatant were then recorded at 540 nm with UV–vis spectrophotometer. The hemolysis rate was calculated according to the following equation:

$$Hemolysis\ (\%) = \frac{A_{sample} - A_1}{A_2 - A_1} \times 100$$

A_{sample} is the absorption of the sample solutions. A_1 is the absorption of PBS, which is confirmed as negative controls. A_2 is the absorption of distilled water, which is confirmed as positive controls.

1.8 Animals

Healthy BALB/c female mice (body weight, 18-22 g) were purchased from the Animal Center of the Second Affiliated Hospital of Harbin Medical University. All animal experiments were performed under the guidelines for Animal Care and Use of Laboratory Animals, following protocols approved by the Institutional Animal Care and Use Committee (IACUC) at the Harbin Medical University, China. The tumor model was generated by subcutaneously injecting 4T1 cancer cells into the flank of

BALB/c mice.

Supporting Figures

Figure S1. Spectra of dehydroabietic acid (DA)

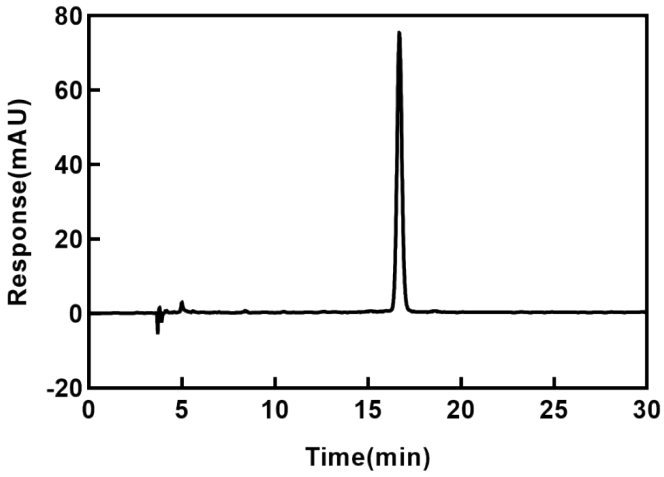

Figure S1-1. Determination of the purity of DA using HPLC.

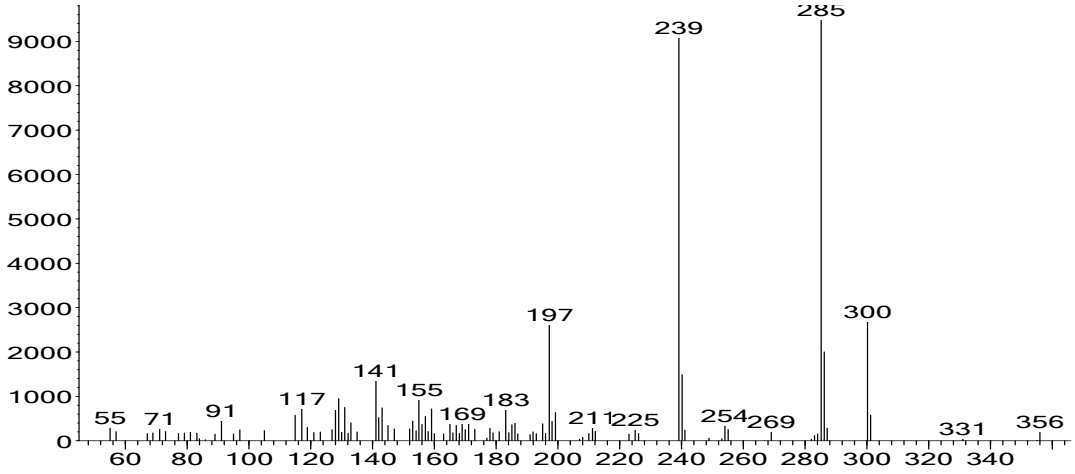

Figure S1-2. GC-MS of DA

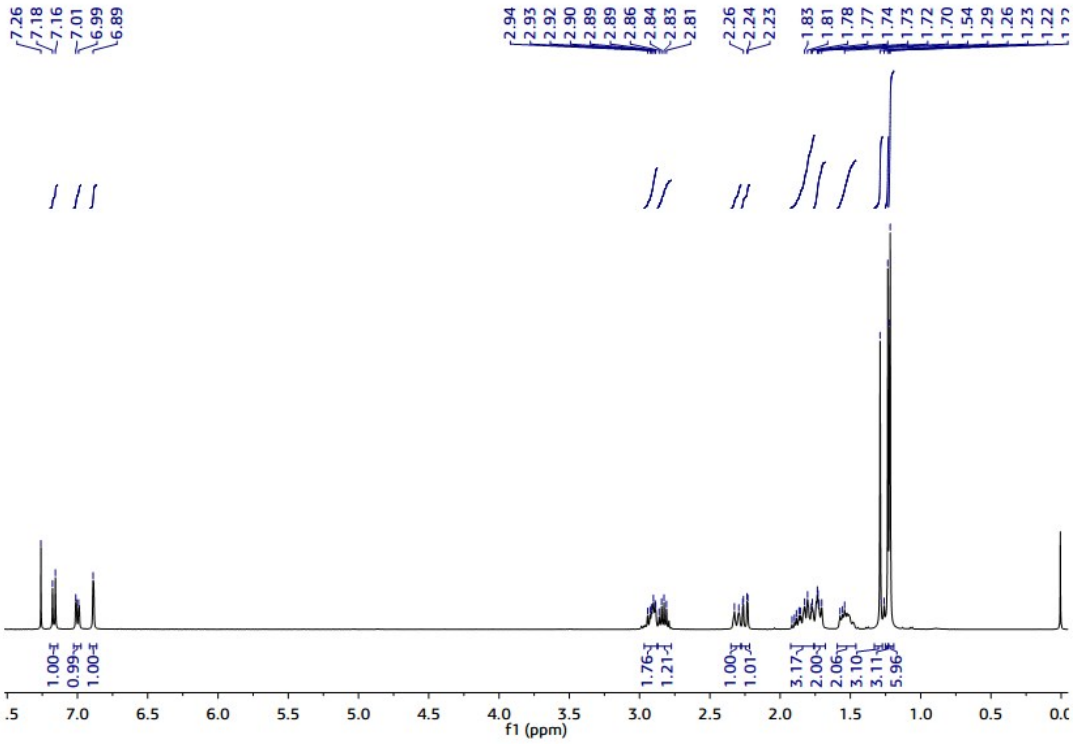

Figure S1-3. ^{1}H-NMR of DA in $CDCl_3$

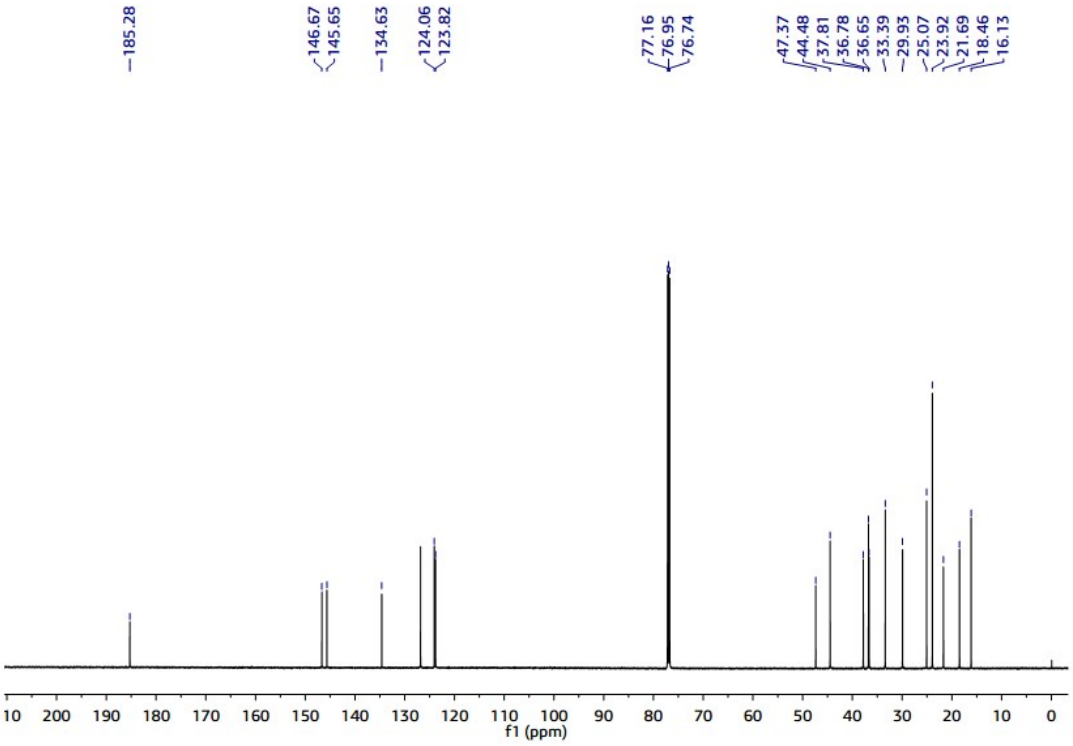

Figure S1-4. ^{13}C-NMR of DA in $CDCl_3$

Figure S2. Spectra of Abietic acid (AA)

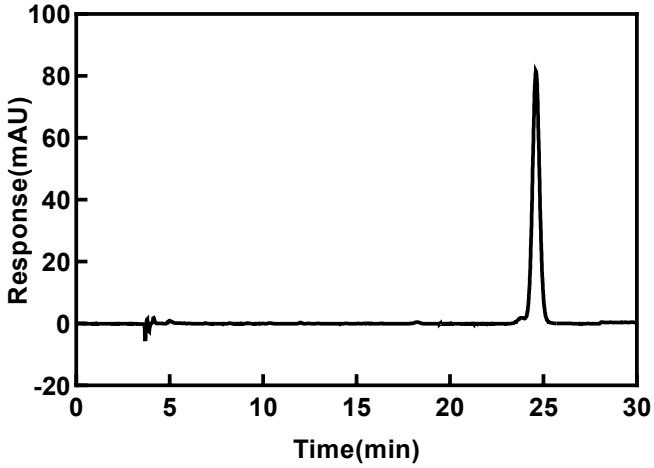

Figure S2-1. Determination of the purity of AA using HPLC.

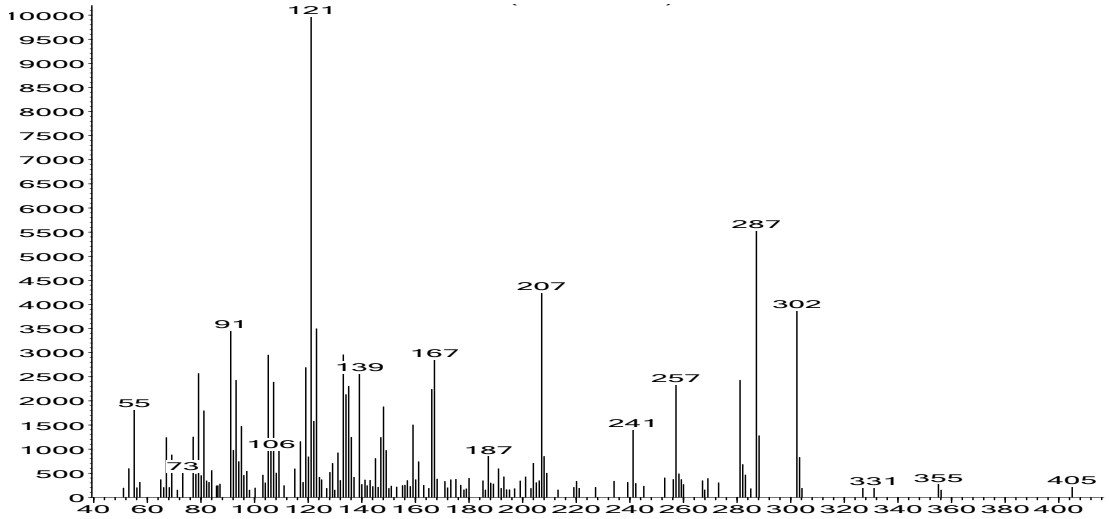

Figure S2-2. GC-MS of AA

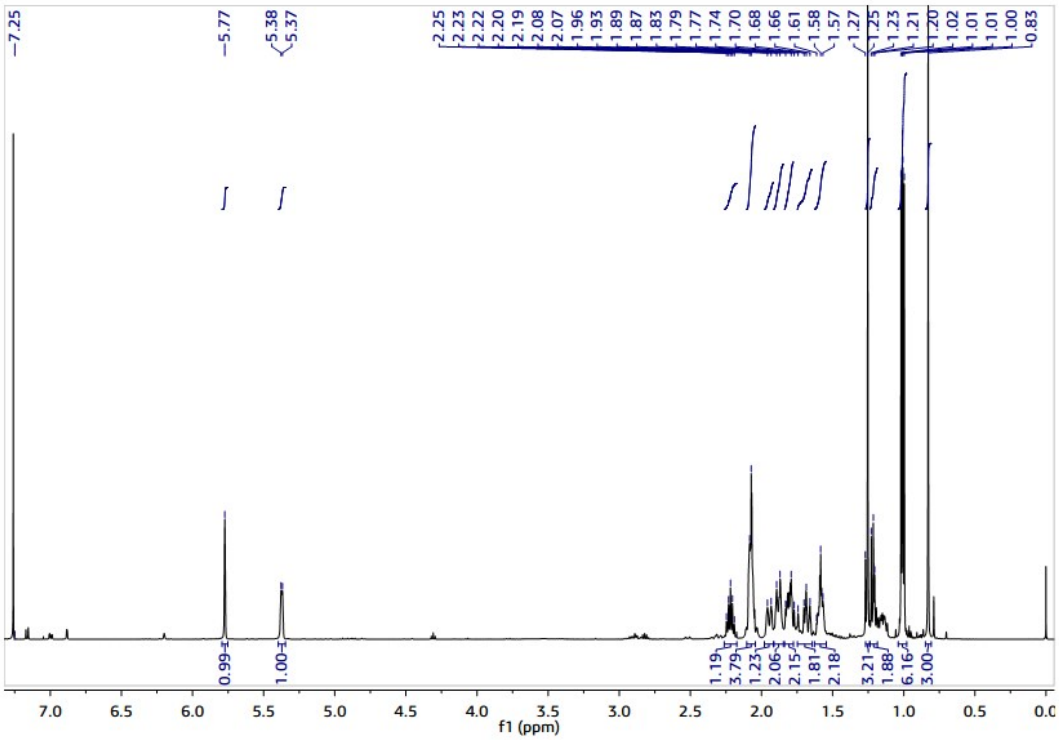

Figure S2-3. ^{1}H-NMR of AA in $CDCl_3$

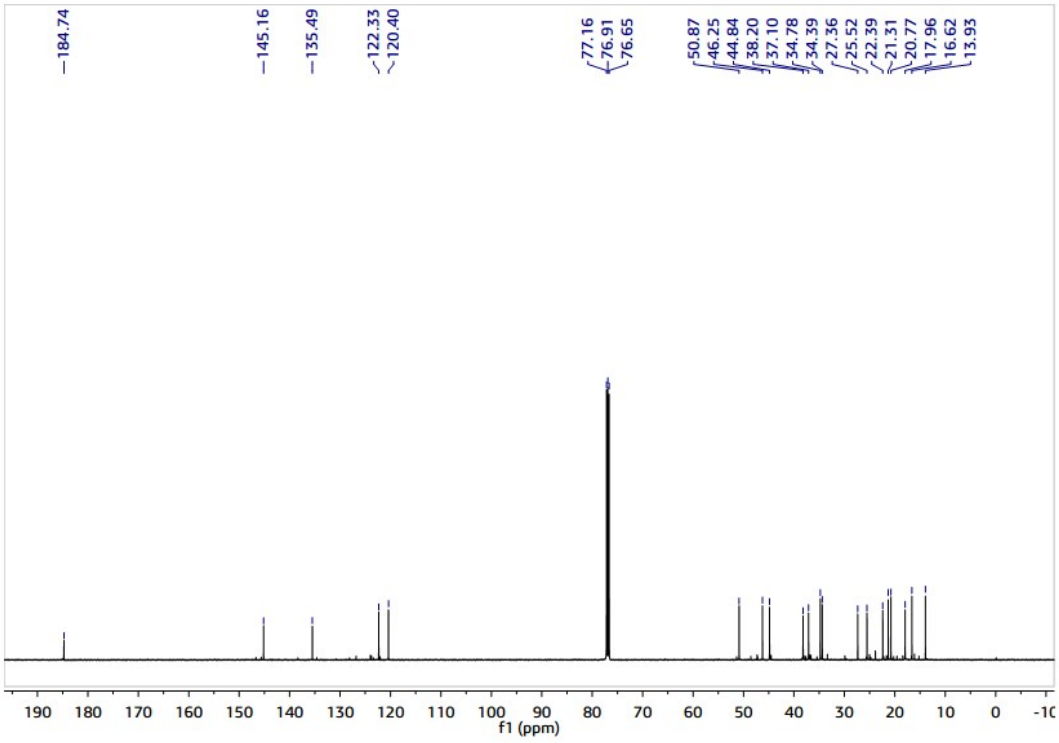

Figure S2-4. ^{13}C-NMR of AA in $CDCl_3$

Figure S3. Spectra of 12-hydroxyabietic acid (12HAA)

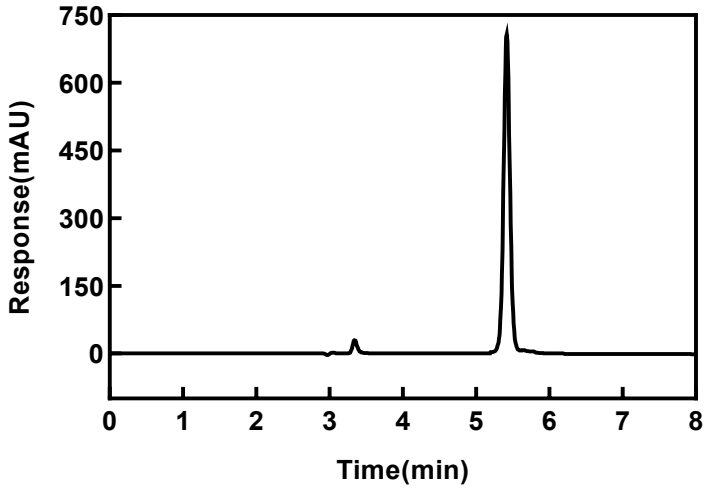

Figure S3-1. Determination of the purity of 12HAA using HPLC.

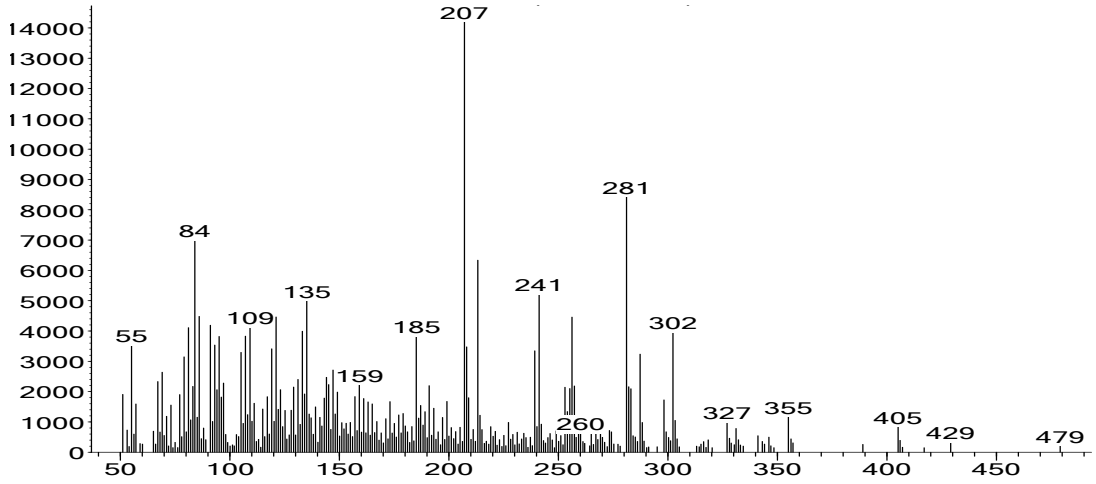

Figure S3-2. GC-MS of 12HAA

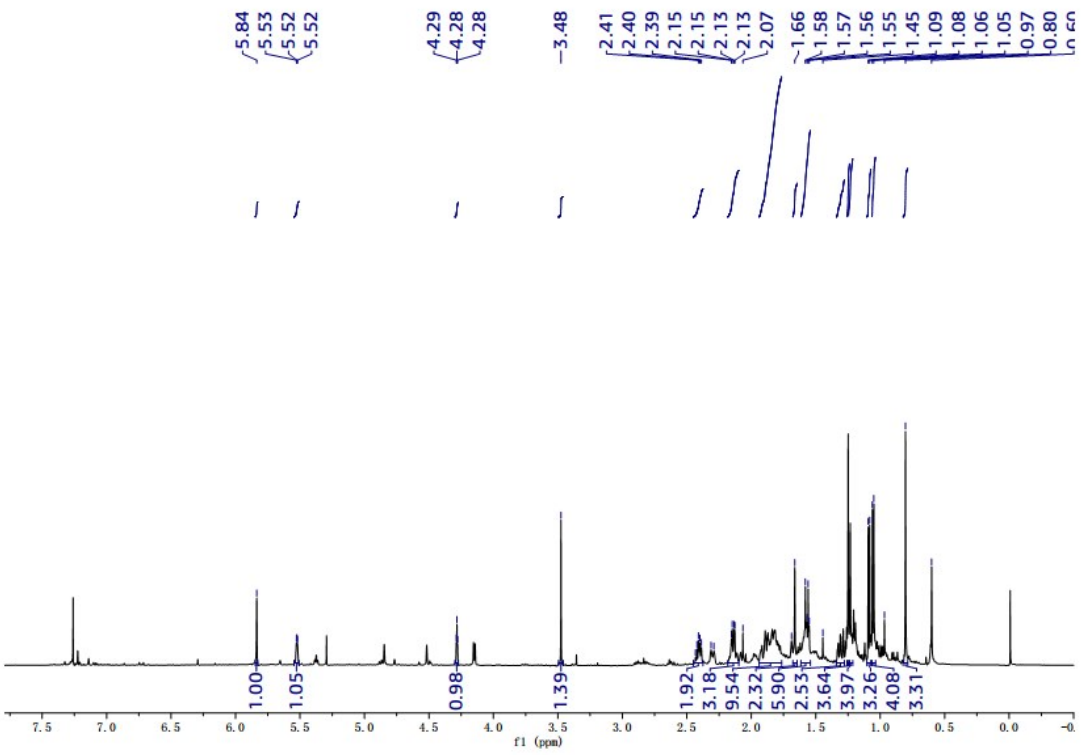

Figure S3-3. ^{1}H-NMR of 12HAA in $CDCl_3$.

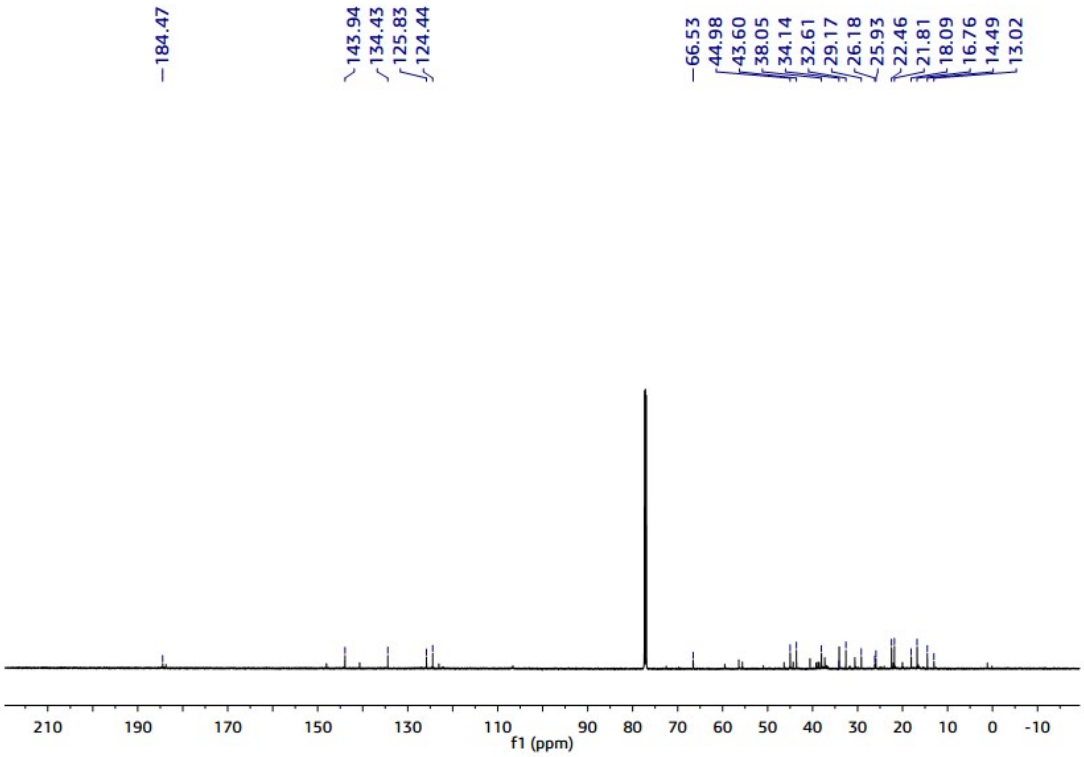

Figure S3-4. ^{13}C-NMR of 12HAA in $CDCl_3$.

Figure S4. Spectra of 15-hydroxyldehydroabietic acid (15HDA)

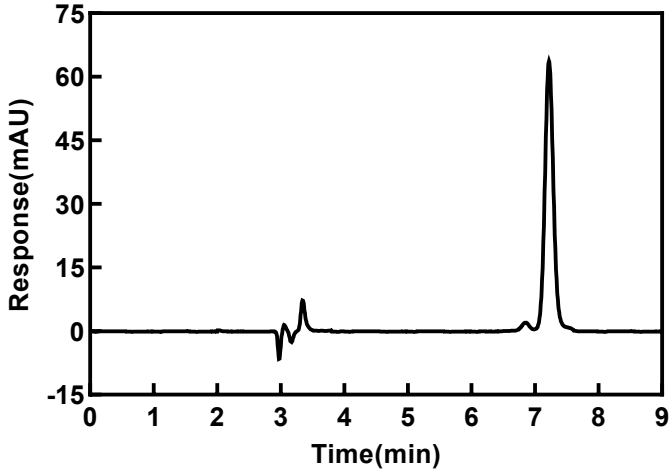

Figure S4-1. Determination of the purity of 15HDA using HPLC.

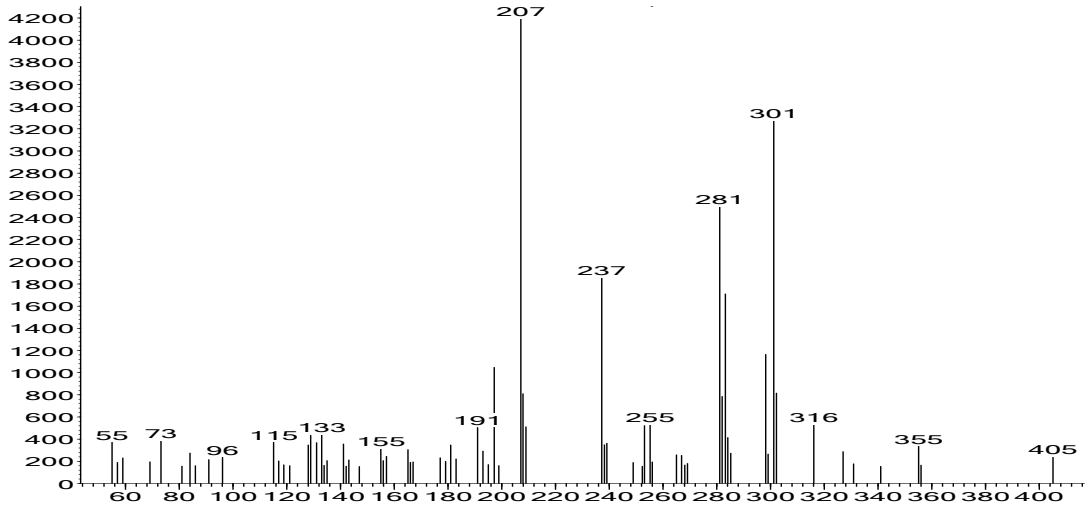

Figure S4-2. GC-MS of 15HDA

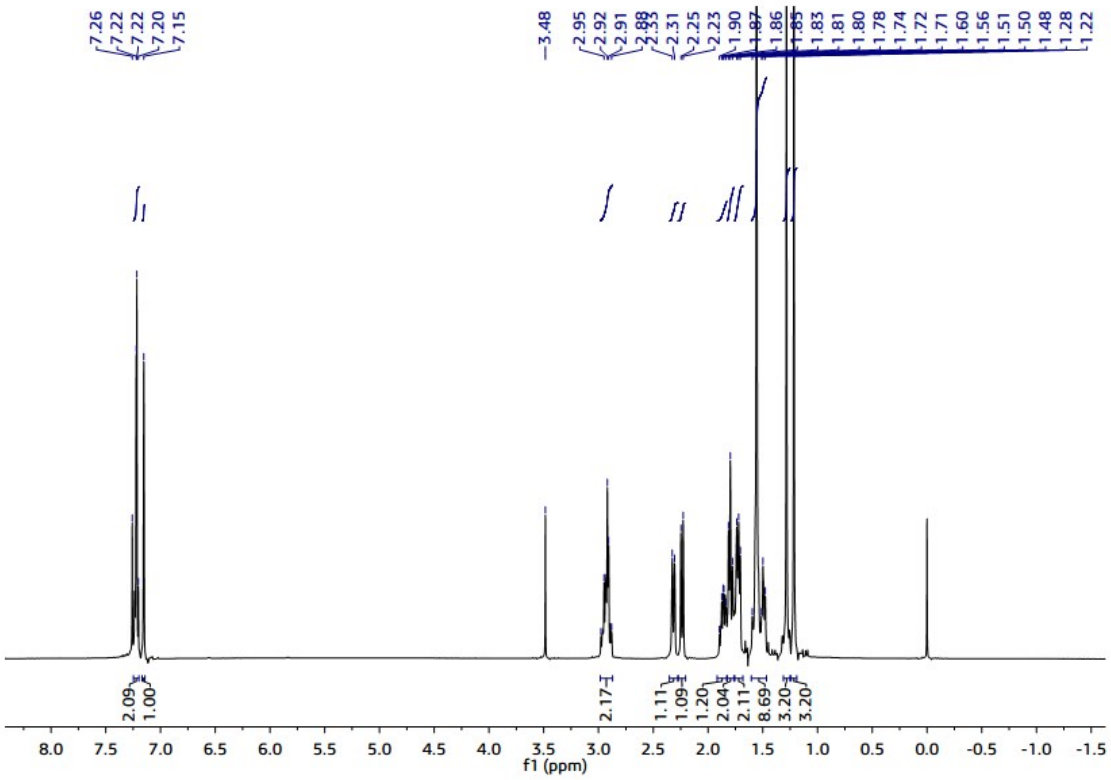

Figure S4-3. ^{1}H-NMR of 15HDA in $CDCl_3$.

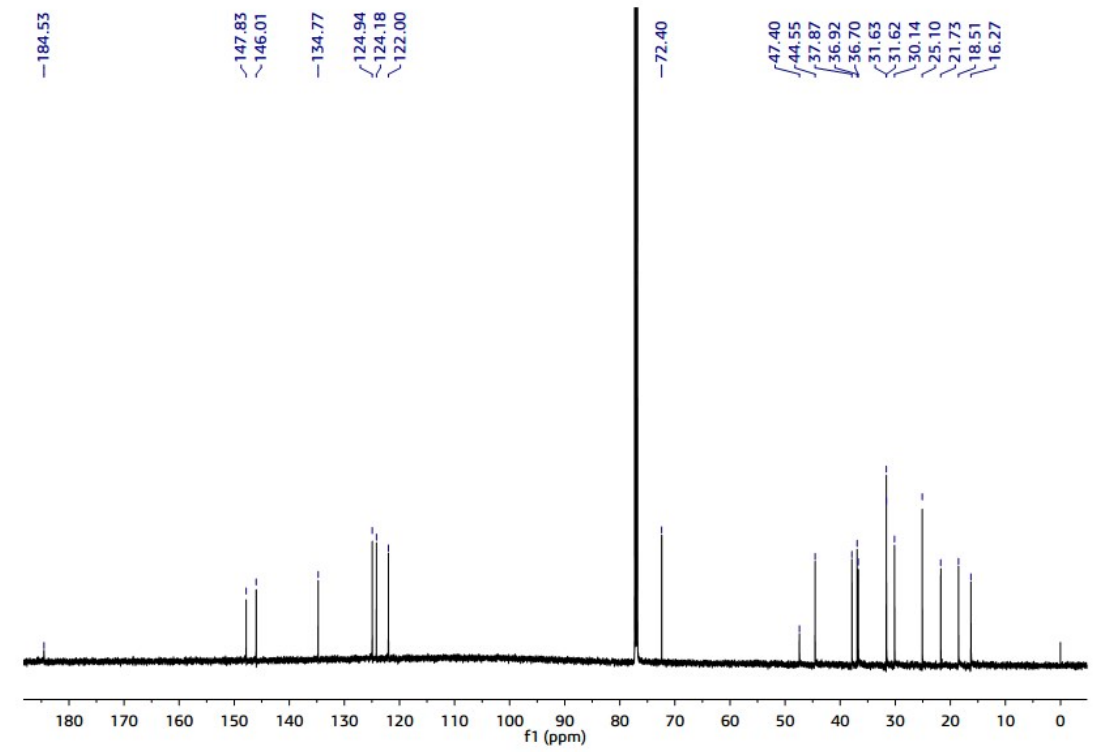

Figure S4-4. ^{13}C-NMR of 15HDA in $CDCl_3$.

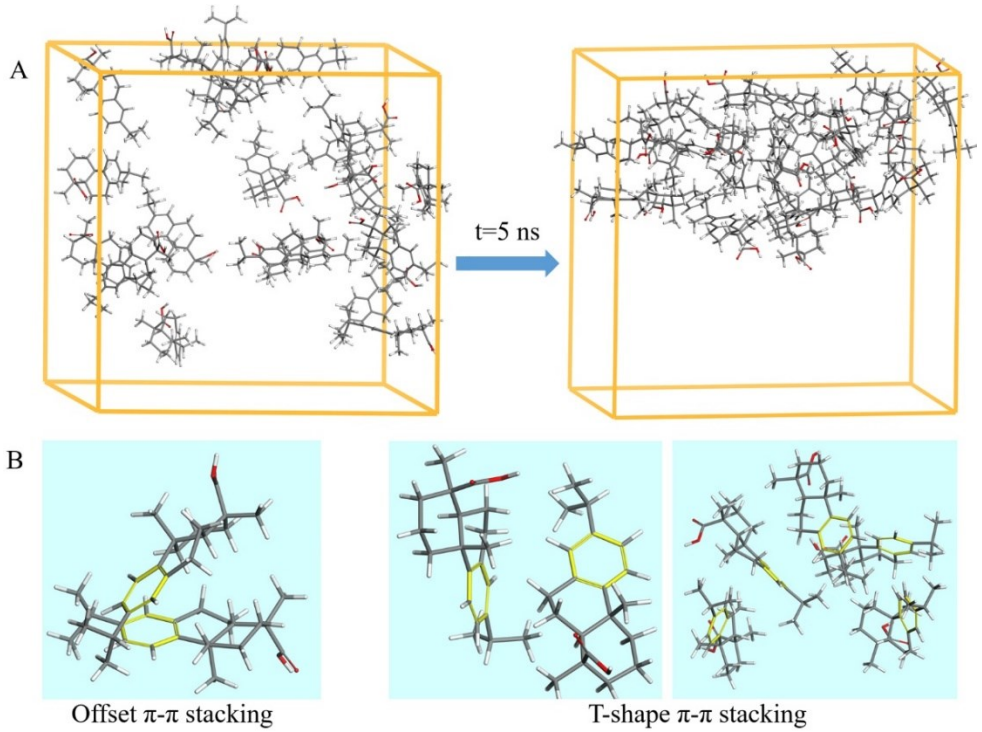

Figure S5. (A) Structure of DA self-assemblies obtained by MD simulation for total 5 ns (5000 ps). Water molecules are omitted. (B) The offset and T-shape π - π stacking among DA molecules were observed in DA self-assemblies.

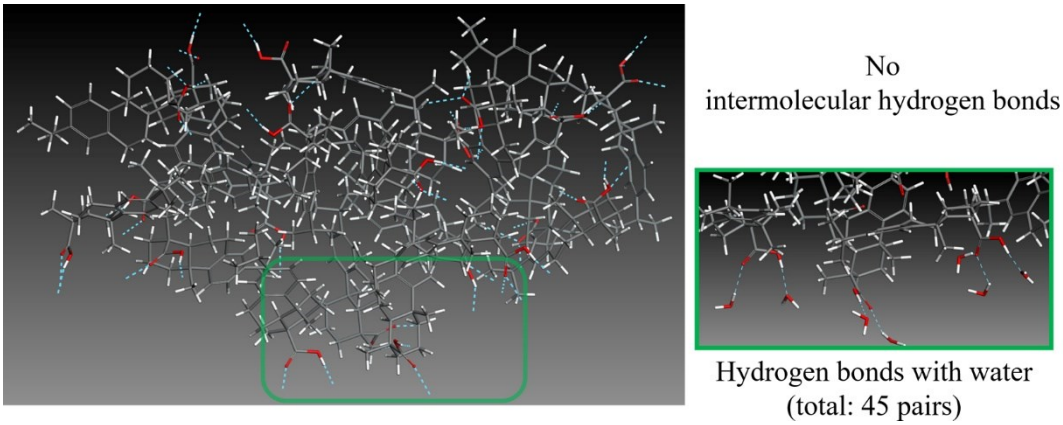

Figure S6. The hydrogen bond information of DA self-assemblies after MD simulation, and water molecules are omitted. There are 45 pairs of hydrogen bonds existing in DA and water molecules. But, no any intermolecular hydrogen bonds among DA molecules could be observed.

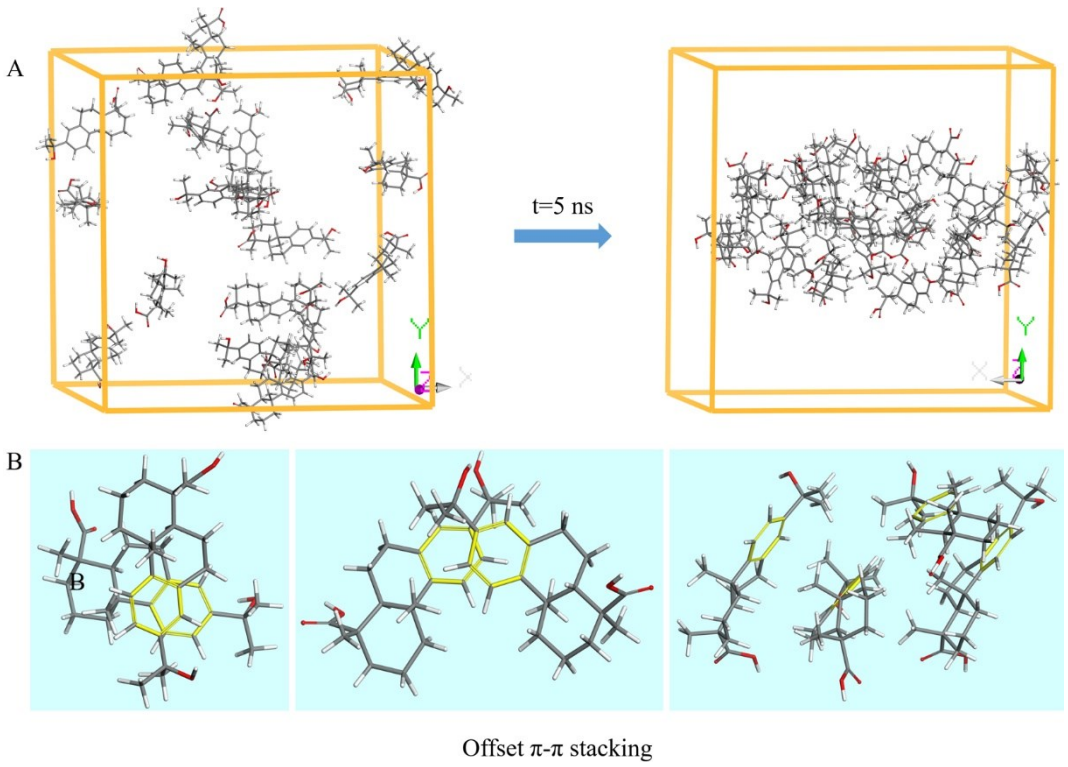

Figure S7. (A) Structure of 15HDA self-assemblies obtained by MD simulation for total 5 ns (5000 ps). (B) A large number of offset π - π stacking among 15HDA molecules could be observed in twenty molecules self-assemblies system. Meanwhile, several 15HDA molecules are arranged in a very regular coplanar manner by π – π stacking, showing a certain regular configuration.

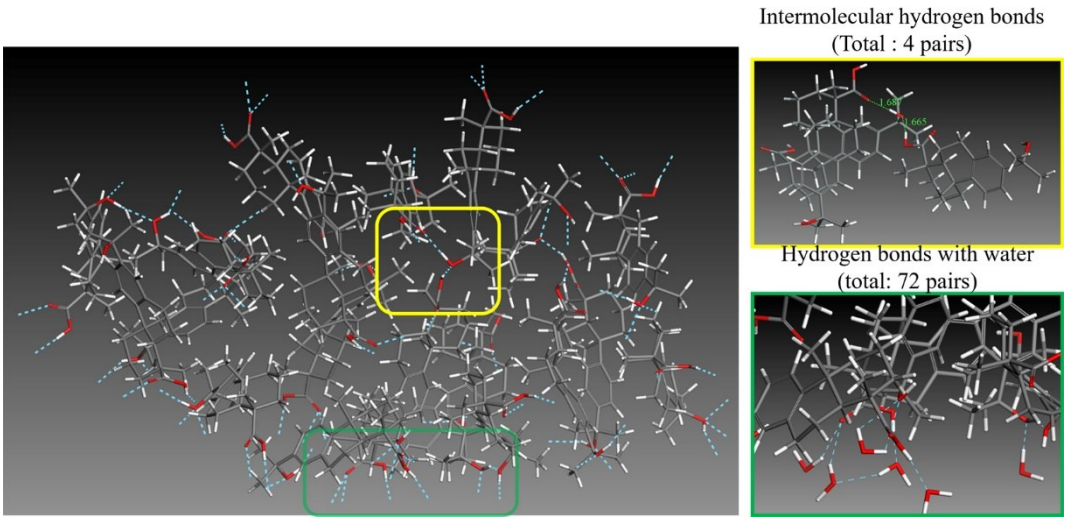

Figure S8. The hydrogen bond information of 15HDA self-assemblies after MD simulation, and corresponding water molecules are omitted. There are 4 pairs of intermolecular hydrogen bonds among 15HDA molecules and 72 pairs of hydrogen bonds between 15HDA and water molecules existing in 15HDA self-assemblies.

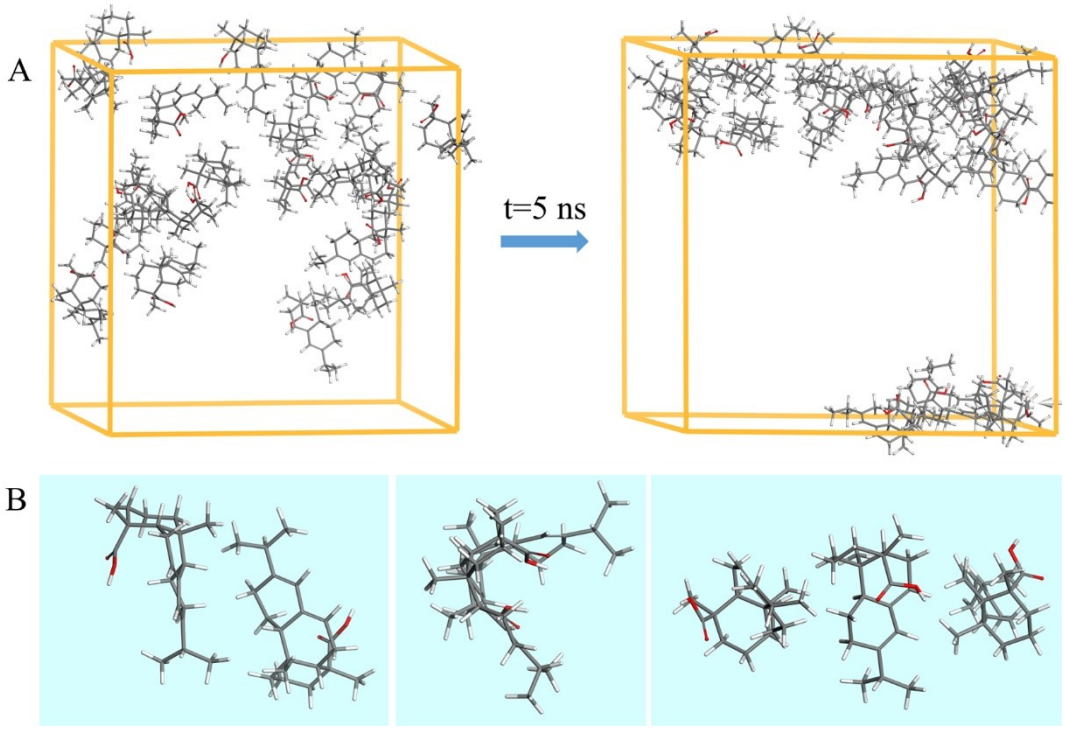

Figure S9. (A) Structure of AA self-assemblies obtained by MD simulation for total 5 ns. (B) AA molecules are arranged in a cross or vertical manner, and no coplanar molecular arrangement was found, showing a disordered configuration.

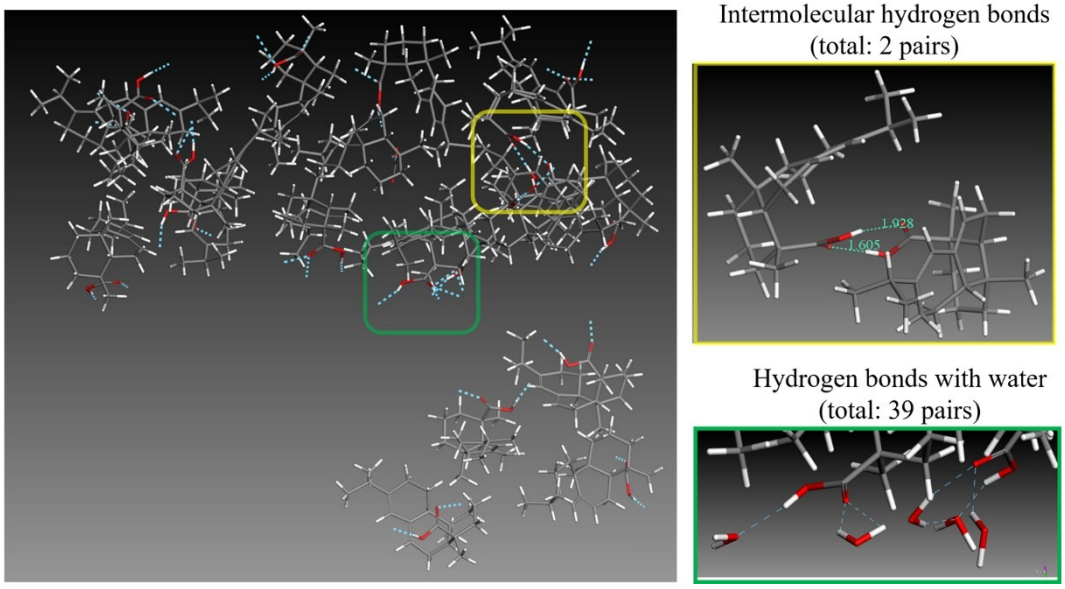

Figure S10. The hydrogen bond information of AA self-assemblies after MD simulation. There are 2 pairs of intermolecular hydrogen bonds among AA molecules and 39 pairs of hydrogen bonds between AA with water molecules existing in AA self-assemblies.

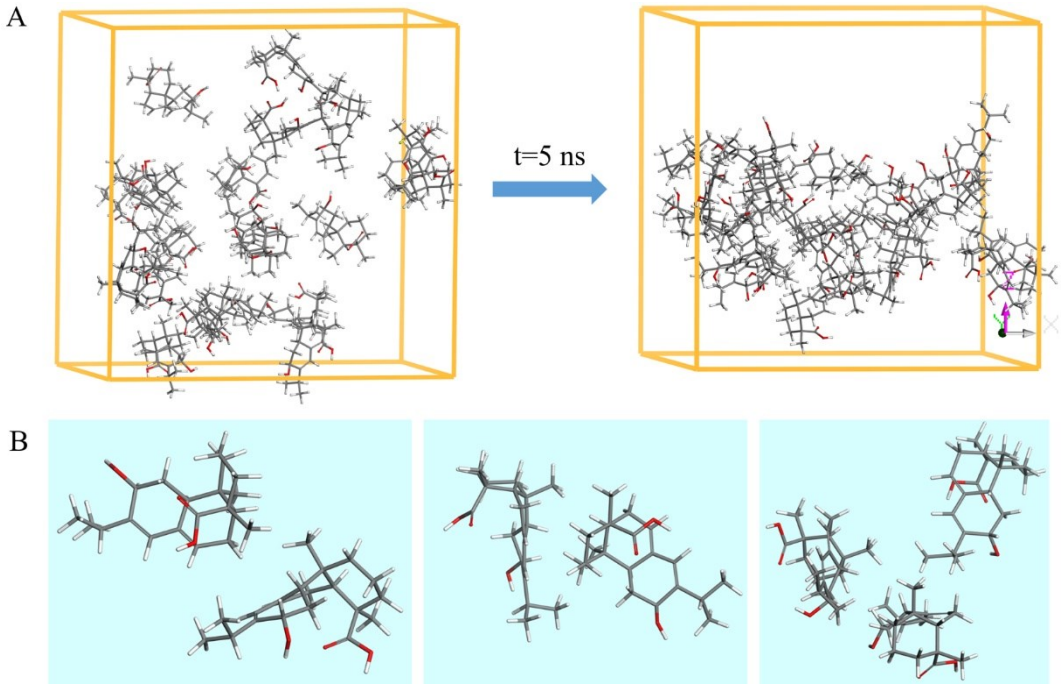

Figure S11. (A) Structure of 12HAA self-assemblies obtained by MD simulation for total 5 ns. (B) 12HAA molecules are also arranged in a cross or vertical manner, and no coplanar molecular arrangement was found, showing a disordered configuration.

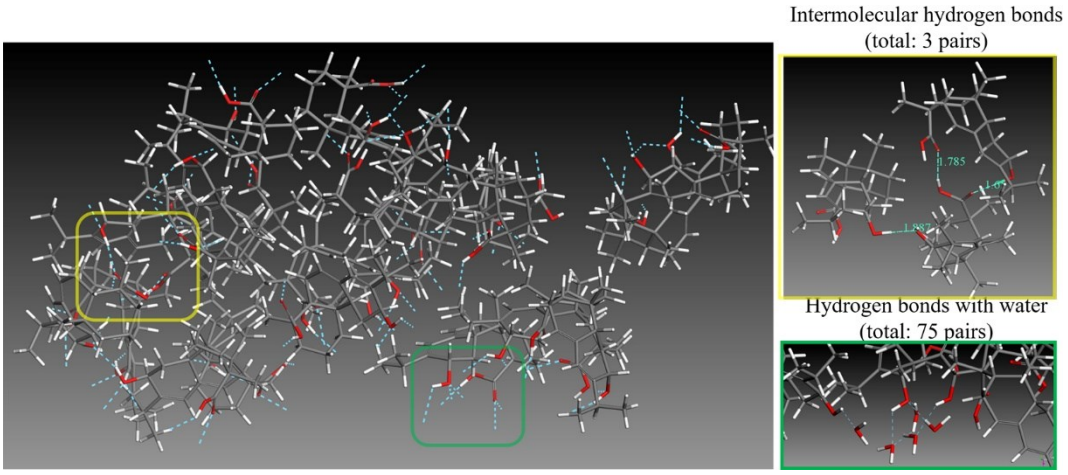

Figure S12. The hydrogen bond information of 12HAA self-assemblies after MD simulation. There are 3 pairs of intermolecular hydrogen bonds among 12HAA molecules and 75 pairs of hydrogen bonds between 12HAA with water molecules existing in 12HAA self-assemblies.

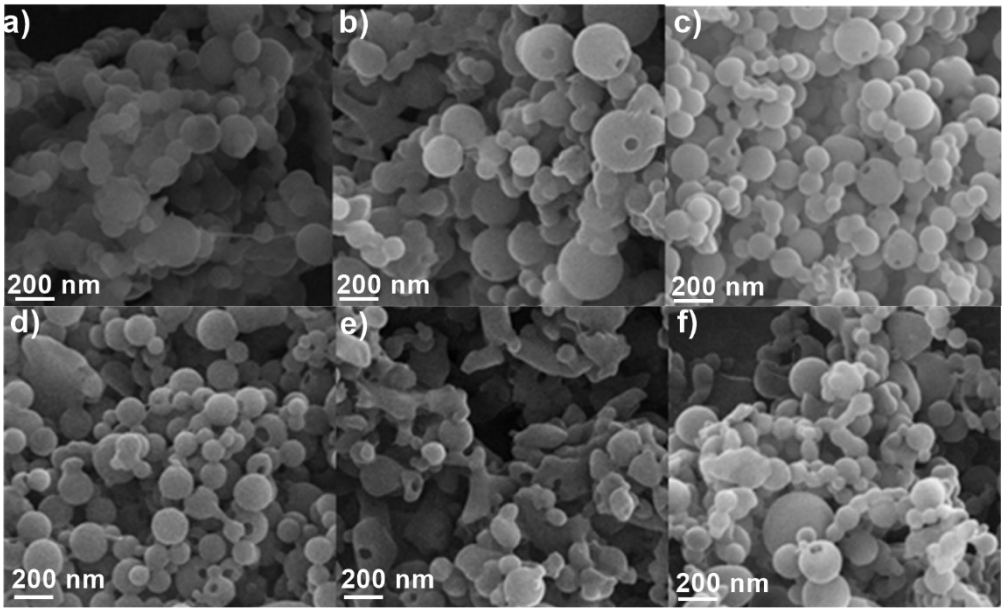

Figure S13. SEM images of AA NPs prepared in different solvents: a) n-hexane, b) cyclohexane, c) dichloromethane, d) chloroform, e) acetic ether, f) acetone.

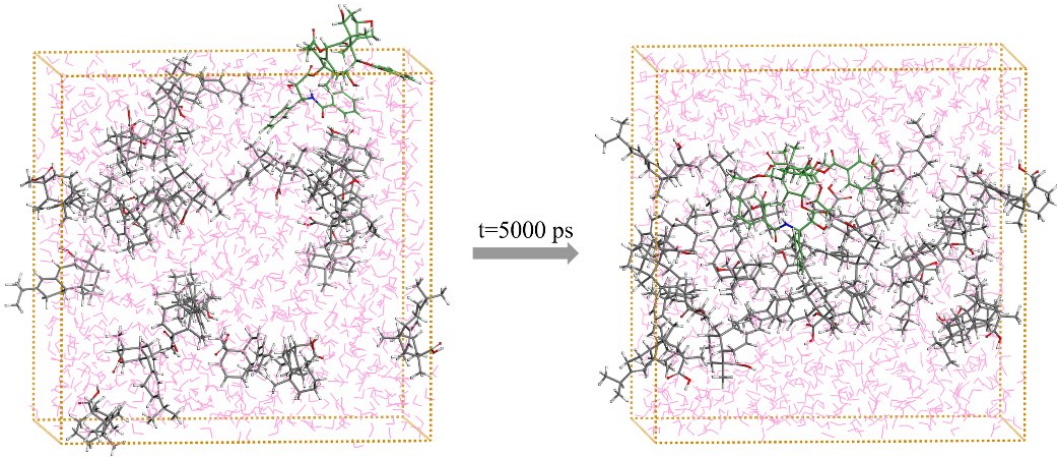

Figure S14. Structure of assembled AA-PTX NPs obtained by MD simulation for total 5 ns. Where the C atoms of PTX are labeled with green. The line and ball models were used for H_2O and AA/PTX molecules, respectively.

Table S1. The diameter (DLS), PDI, Zeta potential of AA NPs prepared in different solvents by emulsion solvent evaporation.

Solvents	Diameter (nm)	PDI	Zeta potential (mV)
n-hexane	317.6	0.292	-29.6±2.96
cyclohexane	301.2	0.237	-27.8±1.83
dichloromethane	259.3	0.185	-23.5±1.99
chloroform	258.4	0.179	-22.7±2.13
ethyl acetate	296.7	0.315	-24.3±2.54
acetone	215.6	0.463	-23.7±2.67

References

1. Gaussian 09, Revision E.01, M. J. Frisch, G. W. Trucks, H. B. Schlegel, G. E. Scuseria, M. A.Robb, J. R. Cheeseman, G. Scalmani, V. Barone, B. Mennucci, G. A. Petersson, H. Nakatsuji, M. Caricato, X. Li, H. P. Hratchian, A. F. Izmaylov, J. Bloino, G. Zheng, J. L. Sonnenberg, M. Hada, M. Ehara, K. Toyota, R. Fukuda, J. Hasegawa, M. Ishida, T. Nakajima, Y. Honda, O. Kitao, H. Nakai, T. Vreven, J. A. Montgomery, Jr., J. E. Peralta, F. Ogliaro, M. Bearpark, J. J. Heyd, E. Brothers, K. N. Kudin, V. N. Staroverov, T. Keith, R. Kobayashi, J. Normand, K. Raghavachari, A. Rendell, J. C. Burant, S. S. Iyengar, J. Tomasi, M. Cossi, N. Rega, J. M. Millam, M. Klene, J. E. Knox, J. B. Cross, V. Bakken, C. Adamo, J. Jaramillo, R. Gomperts, R.E. Stratmann, O. Yazyev, A. J. Austin, R. Cammi, C. Pomelli, J. W. Ochterski, R. L. Martin, K. Morokuma, V. G. Zakrzewski, G. A. Voth, P. Salvador, J. J. Dannenberg, S. Dapprich, A. D. Daniels, O. Farkas, J. B. Foresman, J. V. Ortiz, J. Cioslowski, and D. J. Fox, Gaussian, Inc., Wallingford CT, 2013.